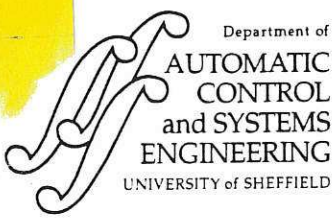

DEVELOPMENT OF A NEURO-ADAPTIVE ACTIVE NOISE CONTROL SYSTEM

M O Tokhi and R Wood

Department of Automatic Control and Systems Engineering,
The University of Sheffield, Mappin Street, Sheffield, S1 3JD, UK.

Tel: + 44 (0)114 282 5136.
Fax: + 44 (0)114 273 1729.
E-mail: O.Tokhi@sheffield.ac.uk.

Research Report No. 679

July 1997

Abstract

This paper presents the development of a neuro-adaptive active noise control (ANC) system. Radial basis function neural networks with an orthogonal forward regression algorithm are considered in both the modelling and control contexts. A feedforward ANC structure is considered for optimum cancellation of broadband noise in a three-dimensional propagation medium. An on-line adaptation and training mechanism allowing a neural-network architecture to characterise the optimal controller within the ANC system is developed. The neuro-adaptive ANC algorithm thus developed is implemented within a free-field environment and simulation results verifying its performance are presented and discussed.

Keywords: *Active noise control, adaptive control, neural networks, orthogonal forward regression, radial basis functions, self-tuning control.*

CONTENTS

LIST OF FIGURES

1 Introduction

Active noise control is realised by artificially generating cancelling source(s), through a process of detection and control, to destructively interfere with the unwanted source and thus result in a reduction in the level of the noise (disturbance) at desired location(s). In this manner, the noise is processed by a suitable electronic controller so that, when superimposed on the disturbance, cancellation occurs (Leitch and Tokhi, 1987).

Noise, in general, is of broadband nature. This requires the control mechanism to realise suitable frequency-dependent characteristics so that cancellation over a broad range of frequencies is achieved (Leitch and Tokhi, 1987). Moreover, in practice, time-varying phenomena, due to variations in the spectral contents of the noise and characteristics of system components, occur. This requires the control mechanism further to be intelligent enough to track these variations, so that the desired level of performance is achieved and maintained (Leitch and Tokhi, 1987; Tokhi and Leitch, 1991a). This paper presents the development of an adaptive ANC mechanism incorporating neural networks.

Much of the work reported on ANC has centred on conventional adaptive controllers (Elliott *et al.*, 1987; Eriksson *et al.*, 1987; Fuller *et al.*, 1992; Ross, 1982; Snyder and Hansen, 1992; Tokhi and Leitch, 1991a). These do not, however, have the long-term memory of intelligent systems to remember the optimal control parameters corresponding to different plant configurations. Intelligent controllers have the ability to sense environment changes and execute the control actions required. Neural networks, on the other hand, have had great success in areas such as speech, natural language processing, pattern recognition and system modelling (Allen, 1987; Lapedes and Farber, 1987; Narendra and Parthasarathy, 1990; Sejnowski and Rosenberg; 1986). Not much work has, however, been reported in the area of intelligent neural-network control applied to ANC systems (Tokhi and Wood, 1995, 1996). This paper attempts to develop an intelligent ANC system incorporating neural networks.

Various types of neural-network architectures have been represented in the literature. Among these the radial basis function (RBF) and the multi-layered perceptron (MLP) networks have commonly been used in the modelling and control of dynamic systems. The

RBF and MLP networks are similar in some respects (Broomhead and Lowe, 1988). The RBF networks, however, can be considered to be superior in many ways to the MLP. The MLP models are highly non-linear in the unknown parameters, and parameter estimation must be based on non-linear optimisation techniques which require intensive computation and which can result in problems associated with local minima. The RBF models do not suffer from such problems. One of the main advantages of the RBF networks is that they are linear in the unknown parameters, and consequently a global minimum in the error surface is achieved. The work presented in this paper utilises RBF networks. This is presented as follows

Section 2 introduces the RBF neural network with its training algorithm and describes the issues involved in the characterisation of dynamic systems using such networks. Section 3 introduces the ANC structure, and presents the development of a neuro-self-tuning ANC system. The development of a simulation environment characterising a free-field medium is presented in Section 4. The neuro-ANC system is implemented within the simulation environment in Section 5, and simulated results of the cancellation of broadband noise achieved with the system are presented and discussed in comparison to an ANC system incorporating the ideal (optimal) controller. Finally, the paper is concluded in Section 6.

2 Radial basis function networks

2.1 Radial basis function models

Radial basis function models can be expressed in the general form of

$$y(t) = f\big(y(t-1),\ldots,y(t-n_y),u(t),u(t-1),\ldots,u(t-n_u),\varepsilon(t-1),\ldots,\varepsilon(t-n_\varepsilon)\big)+\varepsilon(t),$$

where $y(t)$ is the output, $u(t)$ is the input, $\varepsilon(t)$ is the residual and n_y and n_u are the maximum lags in the output and input respectively. The above is known as the Non-linear AutoRegressive Moving Average with eXogenous inputs (NARMAX) model (Leontaritis and Billings, 1985). The NARMAX model can also be expressed by the regression equation

$$y(t) = \sum_{i=1}^{M} p_i(t)\theta_i + \varepsilon(t); \quad t = 1,\ldots,N \tag{1}$$

where $p_i(t)$ are the regressors, $y(t)$ represents the dependent variables, $\varepsilon(t)$ is some modelling error which is uncorrelated with the regressors, θ_i represent the unknown parameters to be estimated, M represents the number of parameters of the regressors and N is the data length. The RBF network can be represented by using the extended model set representation in equation (1) (Billings and Chen, 1989).

An RBF expansion with n inputs and a scalar output implements a mapping according to

$$y(t) = w_o + \sum_{i=1}^{n_r} w_i G(\|\mathbf{x} - c_i\|),$$

where $\mathbf{x}$ is the $n-$dimensional input vector, $G(.)$ is the basis function, $\|.\|$ denotes the Euclidean norm, w_i represent the weights, c_i represent the centres and n_r represents the number of centres. The above mapping can be implemented in a two-layered neural-network structure, where, given fixed centres, the first layer performs a fixed non-linear transformation which maps the input space onto a new space. The output layer implements a linear combiner on this new space. Thus, the RBF expansion can be viewed as a two-layered neural network which has the important property that it is linear in the unknown parameters. Therefore, the problem of determining the parameter values is reduced to one of a linear least-squares optimisation.

Since RBF expansions are linearly dependent on the weights, a globally optimum least-squares interpolation of non-linear maps can be achieved. However, it is important to emphasise that the RBF performance is critically dependent upon the given centres. Although it is known that the fixed centres should suitably sample the input domain, most published results simply assume that some mechanism exists to select centres from data points and do not offer any real means for choosing the centres. The orthogonal forward regression (OFR) algorithm (Korenberg *et al.*, 1988) has been proposed as the mechanism to select the centres and, using the idea of generalisation (Broomhead and Lowe, 1988)

coupled with the model validity techniques, it has been shown that a parsimonious RBF model can be obtained. The centres of the RBF can be chosen from a subset of the input data or boundary within the input and output data values. In practice, only a few significant centres, typically 30 to 50, are required to adequately describe the dynamics of a system. However, when dealing with unknown real systems it is not known which centres are significant. One way of choosing the centres is by using an orthogonal least-squares algorithm (Billings and Chen, 1989). A procedure for selecting appropriate centres for an RBF network using the OFR algorithm has previously been investigated (Chen *et al.*, 1990). The OFR algorithm is used in this investigation to train the RBF network and also select the appropriate centres.

2.2 *The orthogonal forward regression algorithm*

Equation (1) can be written as

$$\mathbf{z} = \mathbf{P}\Theta + \Xi \tag{2}$$

where

$$\begin{aligned} &\mathbf{z} = [z(1) \cdots z(N)]^T, && \mathbf{P} = [\mathbf{p}_1 \cdots \mathbf{p}_M], \\ &\Theta = [\theta_1 \cdots \theta_M]^T, && \Xi = [\xi(1) \cdots \xi(N)]^T, \\ &\mathbf{p}_j = [p_j(1) \cdots p_j(N)]^T; && j = 1,\ldots,M. \end{aligned}$$

An orthogonal decomposition of $\mathbf{P}$ can be obtained as

$$\mathbf{P} = \mathbf{W}\mathbf{A} \tag{3}$$

where

$$\mathbf{A} = \begin{bmatrix} 1 & \alpha_{12} & \alpha_{13} & \cdots & \alpha_{1M} \\ & 1 & \alpha_{23} & \cdots & \alpha_{2M} \\ & & \ddots & & \vdots \\ & & & 1 & \alpha_{M-1M} \\ & & & & 1 \end{bmatrix}$$

is an $M \times M$ unit upper triangular matrix,

$$\mathbf{W} = [\mathbf{w}_1 \quad \cdots \quad \mathbf{w}_M]$$

is an $N \times M$ matrix with orthogonal columns that satisfy $\mathbf{W}^T\mathbf{W} = \mathbf{D}$ and $\mathbf{D}$ is a positive diagonal matrix;

$$\mathbf{D} = \text{diag}\{d_j\}, \quad \text{d}_j = \langle \mathbf{w}_j, \mathbf{w}_j \rangle, \; j = 1, \ldots, M$$

where $\langle .,. \rangle$ denotes the inner product, that is

$$\langle \mathbf{w}_i, \mathbf{w}_j \rangle = \mathbf{w}_i{}^T \mathbf{w}_j = \sum_{t=1}^{N} \text{w}_i(t) w_j(t) .$$

Equation (2) can be rearranged as

$$\mathbf{z} = (\mathbf{P}\mathbf{A}^{-1})(\mathbf{A}\Theta) + \Xi = \mathbf{W}\mathbf{g} + \Xi$$

where $\mathbf{A}\Theta = \mathbf{g}$.

Since $\xi(t)$ is uncorrelated with the regressors,

$$\mathbf{g} = \mathbf{D}^{-1}\mathbf{W}^T\mathbf{z}, \quad g_j = \frac{\langle \mathbf{w}_j, \mathbf{z} \rangle}{\langle \mathbf{w}_j, \mathbf{w}_j \rangle}, \; j = 1, \ldots, M .$$

The number of all the candidate regressors can be very large even though adequate modelling may only require M_s $(<< M)$ significant regressors. The OFR procedure identifies the significant regressors.

The sum of squares of the dependent variable is

$$\langle \mathbf{z}, \mathbf{z} \rangle = \sum_{i=1}^{M} \text{g}_i{}^2 \langle \mathbf{w}_i, \mathbf{w}_i \rangle + \langle \Xi, \Xi \rangle .$$

The error-reduction ratio due to $\mathbf{w}_i$ is thus expressed as the proportion of the dependent variable variance expressed in terms of $\mathbf{w}_i$;

$$[err]_i = \frac{g_i{}^2 \langle \mathbf{w}_i, \mathbf{w}_i \rangle}{\langle \mathbf{z}, \mathbf{z} \rangle} \quad ; \quad 1 \le i \le M .$$

Thus, using equation (3), $\mathbf{W}_s$ is computed, and hence $\mathbf{P}_s$ is obtained from $\mathbf{P}$ using the classical Gram-Schmidt procedure. From the ith stage, by interchanging the i to M

columns of $\mathbf{P}$, a $\mathbf{p}_{ii}$ is selected which gives the largest $[err]_i$ when orthogonalized into $\mathbf{w}_i$. The selection procedure can thus be outlined as

(a) Denote $\mathrm{w}_1^{(i)} = \mathrm{p}_i$; $i = 1,\ldots,M$, and compute

$$g_i^{(i)} = \frac{\langle \mathbf{w}_1^{(i)}, \mathbf{z} \rangle}{\langle \mathbf{w}_1^{(i)}, \mathbf{w}_1^{(i)} \rangle}, \quad [\mathrm{err}]_1^{(i)} = \frac{(g_1^{(i)})^2 \langle \mathbf{w}_1^{(i)}, \mathbf{w}_1^{(i)} \rangle}{\langle \mathbf{z}, \mathbf{z} \rangle}.$$

(b) If $[\mathrm{err}]_1^{(i)} = \max\{[\mathrm{err}]_1^{(i)},\ 1 \le i \le M\}$ is assumed, then $\mathbf{w}_1 = \mathbf{w}_1^{(i)}\ (= \mathbf{p}_i)$ is selected as the first column of $\mathbf{W}_s$ together with the first element of g_s, $g_1 = g_1^{(i)}$, and $[\mathrm{err}]_1 = [\mathrm{err}]_1^{(i)}$.

(c) For the second stage, $i = 1,\ldots,M$, $i \neq j$, and compute

$$\alpha_{12}^{(i)} = \frac{\langle \mathbf{w}_1^{(i)}, \mathbf{z} \rangle}{\langle \mathbf{w}_1^{(i)}, \mathbf{w}_1 \rangle}, \quad \mathbf{w}_2^{(i)} = \mathrm{p}_i - \alpha_{12}^{(i)} \mathbf{w}_1$$

$$g_2^{(i)} = \frac{\langle \mathbf{w}_2^{(i)}, \mathbf{z} \rangle}{\langle \mathbf{w}_2^{(i)}, \mathbf{w}_2^{(i)} \rangle}, \quad [\mathrm{err}]_2^{(i)} = \frac{(g_2^{(i)})^2 \langle \mathbf{w}_2^{(i)}, \mathbf{w}_2^{(i)} \rangle}{\langle \mathbf{z}, \mathbf{z} \rangle}.$$

(d) If $[\mathrm{err}]_2^{(k)} = \max\{[\mathrm{err}]_2^{(i)},\ 1 \le j \le M \text{ and } i \neq j\}$ is assumed, then $\mathbf{w}_2 = \mathbf{w}_2^{(k)}\ (= \mathbf{p}_k - \alpha_{12}\mathbf{w}_1)$ is selected as the second column of W_s together with the second column of A_s, $\alpha_{12} = \alpha_{12}^{(k)}$, the second element of g_s, $g_2 = g_2^{(k)}$, and $[\mathrm{err}]_2 = [\mathrm{err}]_2^{(k)}$.

The error-reduction ratio offers a simple and effective means of selecting a subset of significant regressors from a large number of candidates in a forward regression manner. At the ith step a regressor is selected if it produces the largest value of $[err]_i$ among the number of candidates. The selection procedure is continued until the M_sth stage when

$$1 - \sum_{i=1}^{M_s} [\mathrm{err}]_i < \rho$$

where $0 < \rho < 1$ is a desired tolerance. This leads to a subset of M_s regressors. The parameter estimate $\hat{\Theta}_s$ is then computed from the subset model

$$\mathbf{A}_s \Theta_s = \mathbf{g}_s \tag{4}$$

where $\mathbf{A}_s$ is an upper triangular matrix. The OFR algorithm can thus be outlined as

1. Select the terms of the input vector n_u and n_y.
2. Define the tolerance ρ as a criterion to stop regression.
3. Consider all the p_i's as possible candidates for the significant term. Then, compute the $[err]_i$ values for the p_i and choose the regressor with the largest $[err]_i$ value as the significant term.
4. Compute $1 - \sum_i [err]_i$.
5. If $1 - \sum_i [err]_i > \rho$ then repeat steps 1 to 4 but this time exclude the terms which have been selected from the set of possible candidate terms, p_i.
6. Compute the parameters θ of the final model using equation (4).

2.3 The basis function

Several basis functions have been proposed for the RBF networks (Powell, 1985). These include the linear approximation, cubic approximation, thin-plate-spline, multiquadratic and the inverse multiquadratic functions. Investigations have show that among these the thin-plate-spline function would give the best performance (Jamaluddin, 1991). This function will, thus, be used in this investigation.

2.4 Training considerations

In training an RBF network, the choice of the input vector is important if the network is to capture the dynamics present in the system. The number of input nodes specifies the dimension of the network inputs. Increasing the input dimension of an RBF network does not necessarily improve the network performance. A large input dimension can make the training data appear more distributed. It has been shown that the number of training vectors to cover this space increases exponentially with an increase in the input dimension (Eubank, 1988). A network with an over-specified input dimension gives rise to overlapping decision boundaries, causing the network centres to be sensitive to the region of the input space that is away from the training data. This can result in a network which will be highly sensitive to irrelevant data and give poor generalisation performance.

Theoretical studies have suggested that the network performance can be improved by having a larger number of RBF centres (Powell, 1988). In practice, however, with noise-corrupted data, a network that has an over-assigned number of RBF centres can lead to the problem of overfitting, making the network to give a poor generalisation performance. Whilst the network may give a good output prediction over the data set used in training, it may not provide a good prediction when a different set of data is used.

Theoretical studies have shown that with a larger training sample size a neural network should adapt its structure or complexity (Niyogi and Girosi, 1994). The way to do this is to increase the number of network parameters. This means increasing the flexibility of the network by adjusting the number of centres and input vectors. To avoid overfitting, it is important that an increase in model flexibility should be matched with more training data.

2.5 *Model validation*

To ensure that a fitted neural-network model adequately represents the underlying mechanism which produced the data set, a process of model validation can be employed. Model validity tests are procedures designed to detect the inadequacy of a fitted model.

A common measure of predictive accuracy used in control and system identification is to compute the one-step-ahead (OSA) prediction of the system output. This is expressed as

$$\hat{y}(t) = f\big(u(t), u(t-1), \ldots, u(t-n_u), y(t-1), \ldots, y(t-n_y)\big)$$

where $f(.)$ is a non-linear function, and u and y are the inputs and outputs respectively. The residual or prediction is given by

$$\varepsilon(t-1) = y(t) - \hat{y}(t).$$

Often $\hat{y}(t)$ will be a relatively good prediction of $y(t)$ over the estimation set, even if the model is biased, because the model was estimated by minimising the prediction errors.

Another method of measuring the predictive capability of the fitted model is to compute the model predicted output (MPO). This is defined by

$$\hat{y}_d(t) = f\left(u(t), u(t-1), \ldots, u(t-n_u), \hat{y}_d(t-1), \ldots, \hat{y}_d(t-n_y)\right)$$

with the corresponding deterministic error or residual as

$$\varepsilon_d(t-1) = y(t) - \hat{y}_d(t).$$

If only lagged inputs are used to assign network input nodes then $\hat{y}(t) = \hat{y}_d(t)$.

If the fitted model behaves well for the OSA and the MPO, this does not necessarily imply that the model is unbiased. The prediction over a different set of data often reveals that the model could be significantly biased. One way to overcome this problem is by splitting the data set into two sets, an estimation set and a test set (prediction set). Normally the data set is divided into two halves. The first half is used to train the neural network, and the output is computed. The neural network usually tracks the system output well, and converges to a suitable error minimum. The test set is presented as new inputs to the trained network, and the predicted output is observed. If the fitted model is correct, that is, the number of lagged u's and y's have been correctly assigned, then the network will predict well for the prediction set. In this case the model will capture the underlying dynamics of the system. If both the OSA and the MPO of a fitted model are good over estimation and prediction data sets, then the model is most likely unbiased.

A more convincing method of model validation is to use correlation tests. If a model of a system is adequate, then the residuals or prediction errors $\varepsilon(t)$ should be unpredictable from all linear and non-linear combinations of past inputs and outputs. It has been shown that for an estimated model to be reasonably acceptable and accurate, the following conditions should hold (Billings and Voon, 1986):

$$\begin{aligned}
&\phi_{\varepsilon\varepsilon}(\tau) = E\left[\varepsilon(t-\tau)\varepsilon(t)\right] = \delta(\tau) \\
&\phi_{u\varepsilon}(\tau) = E\left[u(t-\tau)\varepsilon(t)\right] = 0; \ \forall\tau \\
&\phi_{u^2\varepsilon}(\tau) = E\left[\left(u^2(t-\tau) - \overline{u}^2(t)\right)\varepsilon(t)\right] = 0; \ \forall\tau \\
&\phi_{u^2\varepsilon^2}(\tau) = E\left[\left(u^2(t-\tau) - \overline{u}^2(t)\right)\varepsilon^2(t)\right] = 0; \ \forall\tau \\
&\phi_{\varepsilon(\varepsilon u)}(\tau) = E\left[\varepsilon(t)\varepsilon(t-1-\tau)u(t-1-\tau)\right] = 0; \ \tau \geq 0
\end{aligned}$$

where $\phi_{u\varepsilon}(\tau)$ indicates the cross-correlation function between $u(t)$ and $\varepsilon(t)$, $\varepsilon u(t) = \varepsilon(t+1)u(t+1)$ and $\delta(\tau)$ is an impulse function. Ideally the model validity tests

should detect all the deficiencies in network performance, including bias due to internal noise. The cause of the bias will, however, be different for different assignments of network input nodes. Consequently the full five tests defined above should be satisfied.

In practice, normalised correlations are computed. The sampled correlation function between two sequences $\psi_1(t)$ and $\psi_2(t)$ is given by

$$\hat{\phi}_{\psi_1\psi_2}(\tau) = \frac{\sum_{t=1}^{N-\tau} \psi_1(t)\psi_2(t+\tau)}{\sqrt{\sum_{t=1}^{N} \psi_1^2(t) \sum_{t=1}^{N} \psi_2^2(t)}}.$$

Normalisation ensures that all the correlation functions lie in the range $-1 \leq \hat{\phi}_{\psi_1\psi_2}(\tau) \leq 1$ irrespective of the signal strengths. The correlations will never be exactly zero for all lags, and thus the 95% confidence bands defined as $1.96 / \sqrt{N}$, where N is the data length, are used to indicate if the estimated correlations are significant or not. Therefore, if the correlation functions are within the confidence intervals the model is regarded as adequate.

Part of the utility of neural networks comes from their ability to extrapolate from and interpolate between the training data used to set the weights. One way to set the weights of a network to obtain a good generalisation is to use cross-validation. This method uses part of the data as a training set and part as a validation set. One cross-validation method is called 'early stopping'. The network is trained for a while on the validation set, and then tested on the validation set. As training progresses the error on the validation set initially falls. However, the validation error will eventually start to rise when the network is being over-trained. Training is stopped when a minimum of the validation error is reached, even though proceeding might give lower training errors. It is not desirable for a network to be trained to the point where it can faithfully reproduce the training set because it would generalise poorly.

The predictive accuracy of the model can be computed by defining the normalised root mean square of the residuals as an error index:

$$\text{error index} = \sqrt{\frac{\sum(\hat{y}(t) - y(t))^2}{\sum y^2(t)}}.$$

As will be demonstrated later in this paper, the OSA prediction is not a sufficient indicator of model performance because at each step, past inputs, outputs and residuals are used to predict just one increment forward. The MPO, on the other hand, will detect any deficiencies in the fitted model. The OSA prediction and MPO, along with correlation tests, are implemented and used in this work to verify the trained neural-network models.

3 Neuro-active noise control

A schematic diagram of a feedforward ANC structure is shown in Figure 1(a). An unwanted (primary) point source emits broadband noise into the propagation medium. This is detected by a detector, processed by a controller of suitable transfer characteristics and fed to a cancelling (secondary) point source. The secondary signal thus generated is superimposed on the primary signal, so as to achieve cancellation of the noise at and in the vicinity of an observation point. A frequency-domain equivalent block diagram of the ANC structure is shown in Figure 1(b), where E, F, G and H are transfer functions of the acoustic paths between the primary source and the detector, secondary source and the detector, primary source and the observer, and the secondary source and the observer respectively. M, C and L are transfer characteristics of the detector, the observer, the controller and the secondary source respectively. U_D and U_C are the primary and secondary signals at the source locations, whereas Y_{OD} and Y_{OC} are the corresponding signals at the observation point. U_M is the detected signal and Y_O is the observed signal. The control structure in Figure 1 has previously been considered in various noise and vibration control applications (Conover, 1956; Eriksson *et al.*, 1987; Leitch and Tokhi, 1987; Nelson *et al.*, 1987; Ross, 1982; Tokhi and Leitch, 1991a,b,c).

The objective in Figure 1 is to achieve zero noise level at the observation point. This is equivalent to the minimum-variance design criterion in a stochastic environment. This

requires the primary and secondary signals at the observation point to be equal in amplitudes, and to have a phase difference of 180° relative to each other;

$$Y_{OC} = -Y_{OD}. \tag{5}$$

It follows from Figure 1(b) that

$$Y_{OD} = U_D G, \quad Y_{OC} = \frac{U_D EMCL}{1 - FMCL} H. \tag{6}$$

Substituting for Y_{OD} and Y_{OC} from equation (6) into equation (5) and simplifying yields the required controller transfer function as

$$C = \frac{G}{ML(FG - EH)}. \tag{7}$$

Note in equation (7) that, for a given secondary source and detector, the characteristics of the required controller are determined by the transfer characteristics of the acoustic paths from the primary and secondary sources to the detection and observation points. This, in turn, is determined by the geometric arrangement of the system components. Among these, it is possible with some arrangements that the factor $FG - EH$ will be zero or close to zero, requiring the controller to have impractically large gains. Note further in Figure 1 that, with some geometric arrangements of system components, the feedback loop due to the secondary signal reaching the detector can cause the system to become unstable. Therefore, for the system performance to be robust, a consideration of the system in relation to the geometric arrangement of system components is important at the design stage. Such a consideration will allow determination, specifically, of the loci of detection and observation points in the propagation medium that can lead to these problems (Tokhi and Leitch, 1991b,c).

In practice, the characteristics of sources of noise vary due to operating conditions, leading to time-varying spectra. Similarly, the characteristics of transducers, sensors and other electronic equipment used can vary due to environmental effects, ageing, etc. To design an ANC system so that such variations are tracked and the controller characteristics

are updated accordingly, such that the required performance is achieved and maintained, a self-tuning control strategy can be utilised. To realise this, consider the system in Figure 1 with the detected signal, U_M, as input and the observed signal, Y_O, as output. Moreover, owing to the state of the secondary source, let the system be characterised by two sub-systems, namely, when the secondary source is *off*, by an equivalent transfer function denoted by Q_0, and when the secondary source is *on*, by an equivalent transfer function denoted by Q_1;

$$Q_O = \left.\frac{Y_O}{U_M}\right|_{U_C=0} \quad , \quad Q_1 = \left.\frac{Y_O}{U_M}\right|_{U_C\neq 0} \quad . \tag{8}$$

Using the block diagram of Figure 1(b) the detected and observed signals, namely U_M and Y_O can be expressed as

$$\begin{aligned} U_M &= MEU_D + MFU_C \\ Y_O &= GU_D + HU_C \; . \end{aligned} \tag{9}$$

The secondary source signal U_C can be expressed through the controller path as

$$U_C = CLU_M \; . \tag{10}$$

Substituting zero for U_C into equation (9), using equation (8) and simplifying yields the system transfer function Q_0 as

$$Q_O = \frac{1}{M}\left[\frac{G}{E}\right]. \tag{11}$$

Substituting unity for C into equation (10), corresponding to $U_M \neq 0$, and using equations (8) and (9), yields the system transfer function Q_1 as

$$Q_1 = \frac{1}{M}\left[\frac{G}{E}\right] - L\left[\frac{FG-EH}{E}\right]$$

which, after using equation (11) and simplifying, yields

$$ML\left[\frac{FG-EH}{G}\right] = 1 - \frac{Q_1}{Q_O}. \tag{12}$$

The left-hand side of equation (12) is the inverse of the required controller transfer function given in equation (7); hence

$$C = \left[1 - \frac{Q_1}{Q_0}\right]^{-1}. \tag{13}$$

Equation (13) is the required controller design rule expressed in terms of the system transfer characteristics Q_0 and Q_1 which can be measured/estimated on-line. To allow the time-varying phenomena in the system be accounted for, an on-line design and implementation of a neuro-controller can be devised. This can be achieved as

1. obtain the frequency responses of Q_0 and Q_1 using on-line measurement of input/output signals,
2. use equation (13) to obtain the corresponding frequency-response of the (ideal) controller, and
3. train a neural network structure to characterise the ideal controller and implement this on a digital processor.

Moreover, to monitor system performance and update the neuro-controller upon changes in the system, a supervisory-level control can be utilised. This will result in a neuro-self-tuning ANC mechanism. The scheme thus developed is shown in Figure 2, where, 'plant' is the system in Figure 1 between the detection point and the observation point.

To realise the neuro-controller, the topology of the network must be selected. This involves the input data structure and number of centres of the RBF network. Generally, the topology is selected in an intuitive manner, as there are no concrete rules regarding this. This is similar to the selection of model-order in a traditional linear system identification process. The output of the plant is assumed as a non-linear function of its present and past inputs and outputs. This means that the input vector to the network is of the form

$$X(t) = \left[y(t-1),\ldots,y(t-n_y);u(t),u(t-1),\ldots,u(t-n_u)\right]^T$$

where u's and y's represent the inputs and outputs of the plant respectively.

Following the process of structure selection, a neural-network controller is required to be trained to characterise a particular behaviour. One method is to use a conventional controller for the system to produce the training set. In this case, the inputs and their corresponding outputs of the conventional controller are used as the training pairs for the neural network. In this investigation, the ideal controller is used to provide the training data. Thus, the ideal controller is modelled by a neural-network controller. In this process, the OFR algorithm is used to train the network until the global error minimum is reached.

4 Development of the simulation environment

To allow development of a suitable simulation environment for test and verification of the control strategy, consider a loudspeaker with its drive amplifier, and a microphone incorporating its pre-amplifier located at a set distance r_m in front of the loudspeaker. This is shown in an equivalent block diagram in Figure 3 where

L = Transfer characteristics of the loudspeaker.

M = Transfer characteristics of the microphone.

$\frac{A}{r_m} exp(-j r_m \omega / c)$ = The characteristics of the acoustic path through r_m with A as a constant, c as the speed of sound and ω the radian frequency. Note that the acoustic medium is assumed to be non-dispersive.

Let the amplitude and phase response of the system in Figure 3 from the input of the loudspeaker to the output of the microphone as a function of the frequency ω be denoted by A_m and Q_m respectively;

$$A_m \exp(jQ_m) = ML \frac{A}{r_m} \exp(-j r_m \omega / c). \qquad (14)$$

The frequency responses of the acoustic paths in Figure 1 can be written as

$$
\begin{aligned}
E(j\omega) &= (A/r_e)\exp(-j\, r_e\omega/c) \\
F(j\omega) &= (A/r_f)\exp(-j\, r_f\omega/c) \\
G(j\omega) &= (A/r_g)\exp(-j\, r_g\omega/c) \\
H(j\omega) &= (A/r_h)\exp(-j\, r_h\omega/c)
\end{aligned}
\qquad (15)
$$

where r_e, r_f, r_g and r_h represent the distances of the acoustic paths between the primary source and the detector, the secondary source and the detector, the primary source and the observer, and the secondary source and the observer respectively. Let E', F', G' and H' be transfer characteristics defined as

$$
\begin{aligned}
E' &= MLE = A_e \exp(jQ_e) \\
F' &= MLF = A_f \exp(jQ_f) \\
G' &= MLG = A_g \exp(jQ_g) \\
H' &= MLH = A_h \exp(jQ_h)\,.
\end{aligned}
\qquad (16)
$$

Using equations (14), (15) and (16) yields

$$
\begin{aligned}
A_e &= A_m(r_m/r_e), \quad Q_e = Q_m - (r_e - r_m)\omega/c \\
A_f &= A_m(r_m/r_f), \quad Q_f = Q_m - (r_f - r_m)\omega/c \\
A_g &= A_m(r_m/r_g), \quad Q_g = Q_m - (r_g - r_m)\omega/c \\
A_h &= A_m(r_m/r_h), \quad Q_h = Q_m - (r_h - r_m)\omega/c\,.
\end{aligned}
\qquad (17)
$$

Thus, using equation (17) with given data for A_m and Q_m, the frequency responses E', F', G' and H' can be obtained with different arrangements of the primary source, secondary source, detector and observer locations using the corresponding values for r_e, r_f, r_g and r_h. This results in an equivalent block diagram of the ANC system as shown in Figure 4. Signal propagation through the system in Figure 1 can thus be simulated by using the block diagram in Figure 4, either in the frequency domain or in the time-domain. The frequency-domain approach will require the frequency responses of the system components, as obtained through the procedure outlined above. The time-domain approach will, however, require transformation of the frequency responses obtained above into the time-domain, using an inverse Fourier transformation. This gives the corresponding impulse responses of the system components, which can be used within convolution relations to obtain the required signals through the system. Note that the accuracy of the results

depends on the size of the data window; the larger the window the more accurate the results will be. The time-domain approach is preferred in this work, since subsequent investigations into the training of neural networks will require signals in the time domain.

5 Implementations and results

To realise the ANC simulation environment, an experiment was conducted using the arrangement shown in Figure 3 with $r_m = 0.03$ metres. A sine wave of fixed amplitude and phase was fed into the power amplifier and the frequency varied over the range $0 - 500$ Hz. The amplitude and phase of the microphone output was measured relative to the input, and recorded to enable the gain and phase of the system be obtained. The gain and phase relationships of the system thus measured are shown in Figure 5.

The simulation algorithm was coded using MATLAB and implemented on a 486 PC. A pseudo-random binary sequence (PRBS) simulating a broadband signal in the range $0 - 500$ Hz was utilised as the primary noise source. The system components were arranged with the observer at 1.5 metres away and equidistant from the primary and secondary sources. With the values of the distances r_e, r_f, r_g and r_h set, the transfer characteristics and corresponding impulse responses of system components in the block diagram of Figure 4 were obtained. The corresponding amplitude and phase characteristics of the controller for optimum cancellation at the observation point are shown in Figure 6. It is noted that the ideal controller has a flat amplitude characteristic throughout the frequency range, except at frequencies below 40 Hz, where it has a large gain. This is due to the similarly large attenuation in the loudspeaker characteristics, see Figure 5. The phase characteristics of the controller, on the other hand, have a rising feature as a function of frequency.

To obtain the amount of cancellation achieved with the ideal controller over a broad frequency range of the noise, the autopower spectral densities of the noise before and after cancellation and the corresponding difference, that is, the cancelled spectrum was obtained.

This is shown in Figure 7. It is seen that an average of 20 dB cancellation was achieved over the broad frequency range of the noise.

Note that, with the system employing the ideal controller, the amount of cancellation achieved should be infinity. However, due to the level of accuracy attainable with the computing domain and the size of the data window utilised, the results shown are the best obtainable under these circumstances. Thus, for purposes of this investigation, these will be used subsequently for verification of performance of the neuro-ANC system.

To implement the RBF neuro-controller a network with 65 centres and input vector with $n_u = n_y = 15$ was set up. These parameters were arrived at through the model validation tests described in Section 2. The input and the corresponding output of the ideal controller were used as the training pair with the OFR algorithm and the thin-plate-spline as the basis function for the RBF network. Both the OSA prediction and the MPO were used to train the network. One half of the data was used as the estimation set and the remaining half was used as the test set. Later, the full data set was used to train the network and evaluate the system performance in comparison to the ideal controller.

Figure 8 shows the OSA prediction and MPO of the network, achieving error indices of 0.0002 and 0.0002 for the estimation set and 0.0031 and 0.0045 for the test set respectively. Note that the estimation set error of the MPO is at a similar level as compared to that of the OSA prediction. The test set shows a larger error in the output with the MPO in comparison to the OSA prediction. Although, the test set error in each case is relatively larger than the estimation-set error, the network gives a good output prediction. The corresponding correlation test functions were all found to be within the 95% confidence intervals, indicating an adequately fitted model.

To train the network for utilisation in the ANC system, the full data set was used in the training procedure. The network achieved a predicted output with an error index of 0.0002. The performance of the ANC system was monitored at the observation point with the neuro-controller. Figure 9 shows the cancelled spectrum thus obtained. It is noted that an average level of around 20 dB cancellation has been achieved with the neuro-controller. This is similar to the performance achieved with the ideal controller, see Figure 7.

6 Conclusion

The development of a neuro-adaptive ANC system has been presented and verified in the cancellation of broadband noise in a three-dimensional propagation medium.

An RBF neural network with an OFR algorithm for training the network has been introduced. The capability of the network in characterising dynamic systems has been investigated. Both the OSA prediction and the MPO have been used as the training methods. It has been shown that with a suitable choice of the input data structure the system data can be faithfully predicted with an acceptable prediction error minimum.

A feedforward ANC structure has been considered for optimum cancellation of broadband noise at an observation point in a three-dimensional propagation medium. The controller design relations have been formulated so as to allow on-line design and implementation, and hence a self-tuning control algorithm. The RBF neural network has been incorporated within the algorithm to characterise the optimal controller. In this manner, a self-tuning neuro-ANC system has been introduced for broadband noise cancellation. This has incorporated a supervisory level of control which detects variations in the system and enables the controller characteristics to be updated, so as to achieve and maintain the desired level of system performance. The neuro-adaptive ANC algorithm thus developed has been tested within an acoustic environment characterising a non-dispersive propagation medium, and its performance was verified in the cancellation of broadband noise in comparison to the idea controller. It has been shown that the neuro-ANC system achieves as good a performance as the system incorporating the ideal controller.

7 References

Allen, R. B. (1987). Several studies on natural language and backpropagation, *Proceedings of IEEE First International Conference on Neural Networks*, San Diego, **2**, 335-341, 1987.

Billings, S. A. and S. Chen (1989). Extended model set, global data and threshold model identification of severely nonlinear systems, *International Journal of Control*, **50** (5), 1897-1923.

Billings, S. A. and W. S. F. Voon (1986). Correlation based model validity tests for non-linear systems, *International Journal of Control*, **15** (6), 601-615.

Broomhead, D. S. and D. Lowe (1988). Multivariable functional interpolation and adaptive networks, *Complex Systems*, **2**, 321-355.

Chen, S., C. F. N. Cowen, S. A. Billings and P.M. Grant (1990). Practical identification of NARMAX models using radial basis functions, *International Journal of Control*, **52** (6), 1327-1350.

Conover, W. B. (1956). Fighting noise with noise, *Noise Control*, **2** (2), 78-82 & 92.

Elliott, S. J., I. M. Sothers and P.A. Nelson (1987). A multiple error LMS algorithm and its application to the active control of sound and vibration, *IEEE Transactions on Acoustics, Speech, and Signal Processing*, **35** (10), 1423-1434.

Eriksson, L. J., M. C. Allie and R. A. Greiner (1987). The selection and application of an IIR adaptive filter for use in active sound attenuation, *IEEE Transactions on Acoustics, Speech, and Signal Processing*, **35** (4), 433-437.

Eubank, R. (1988). *Spline smoothening and nonparametric regression*, Marcel Dekker, London.

Fuller, C. R., C.A. Rogers and H. H. Robertsaw (1992). Control of sound radiation with active/adaptive structures, *Journal of Sound and Vibration*, **157** (1), 19-39.

Jamaluddin, H. B. (1991). *Nonlinear system identification using neural networks*, PhD thesis, Department of Automatic Control and Systems Engineering, The University of Sheffield, UK.

Korenberg, M. J., S. A. Billings, Y. P. Liu and P. J. McIlroy (1988). Orthogonal parameter estimation algorithm for nonlinear stochastic systems, *International Journal of Control*, **48** (1), 193-210.

Lapedes, A. and R. Farber (1987). *Nonlinear signal processing using neural networks: Prediction and system modelling*,' Preprint LA-UR-87-2662, Los Alamos National Laboratory, Los Alamos.

Leitch, R. R. and M. O. Tokhi (1987). Active noise control systems, *IEE Proceedings-A*, **134** (6), 525-546.

Leontaritis, I. J., and S. A. Billings (1985). Input-output parametric models for nonlinear systems, Part I: Deterministic nonlinear systems; Part II: Stochastic nonlinear systems, *International Journal of Control*, **41** (2), 303-344.

Narendra, K. S. and K. Parthasarathy (1990). Identification and control of dynamical systems using neural networks, *IEEE Transactions on Neural Networks*, **1** (1), 4-27.

Nelson, P.A., A. R. D. Curtis, S. J. Elliott and A. J. Bullmore (1987). The active minimization of harmonic enclosed sound fields, Part I: Theory, *Journal of Sound and Vibration*, **117** (1), 1-13.

Niyogi, P. and F. Girosi (1994). *On the relationship between generalisation error, hypothesis complexity, and sample complexity for radial basis functions*, A. I. Memo 1467, Artificial intelligence laboratory, MIT, Massachusetts.

Powell, M. J. D. (1985). Radial basis functions for multivariable interpolation: A review, *Proceedings of the IMA Conference on Algorithms for the Approximation of Functions and Data*, RMCA, Shrivenham.

Powell, M. J. D. (1988). Radial basis function approximations to polynomials, *Numerical Analysis 1987 Proceedings* , Dundee, 223-241.

Ross, C.F. (1982). An adaptive digital filter for broadband active sound control, *Journal of Sound and Vibration*, **80** (3), 381-388.

Sejnowski, T. J. and C. R. Rosenberg (1986). *NETtalk: A parallel network that learns to read aloud*,. Technical Report JHU/EECS-86/01, Johns Hopkins University USA.

Snyder, S. D. and C. H. Hansen (1992). Design consideration for active noise control systems implementing the multiple input, multiple output LMS algorithm, *Journal of Sound and Vibration*, **159** (1), 157-174.

Tokhi, M. O. and R. R. Leitch (1991a). Design and implementation of self-tuning active noise control system, *IEE Proceedings-D*, **138** (5), 421-430.

Tokhi, M. O. and R. R. Leitch (1991b). Design of active noise systems operating in three-dimensional non-dispersive propagation medium. *Noise Control Engineering Journal*, **36** (1), 41-53.

Tokhi, M. O. and R. R. Leitch (1991c). The robust design of active noise control systems based on relative stability measures. *The Journal of The Acoustical Society of America*, **90** (1), 334-345.

Tokhi, M. O. and R. Wood (1995). Active control of noise using neural networks, *Proceedings of the Institute of Acoustics*, **17** (Part 4), 209-216.

Tokhi, M. O. and R. Wood (1996). Radial basis function neuro-active noise control, *Preprints of IFAC-96: 13th World Congress*, San Francisco, 30 June-05 July 1996, **K**, 97-102.

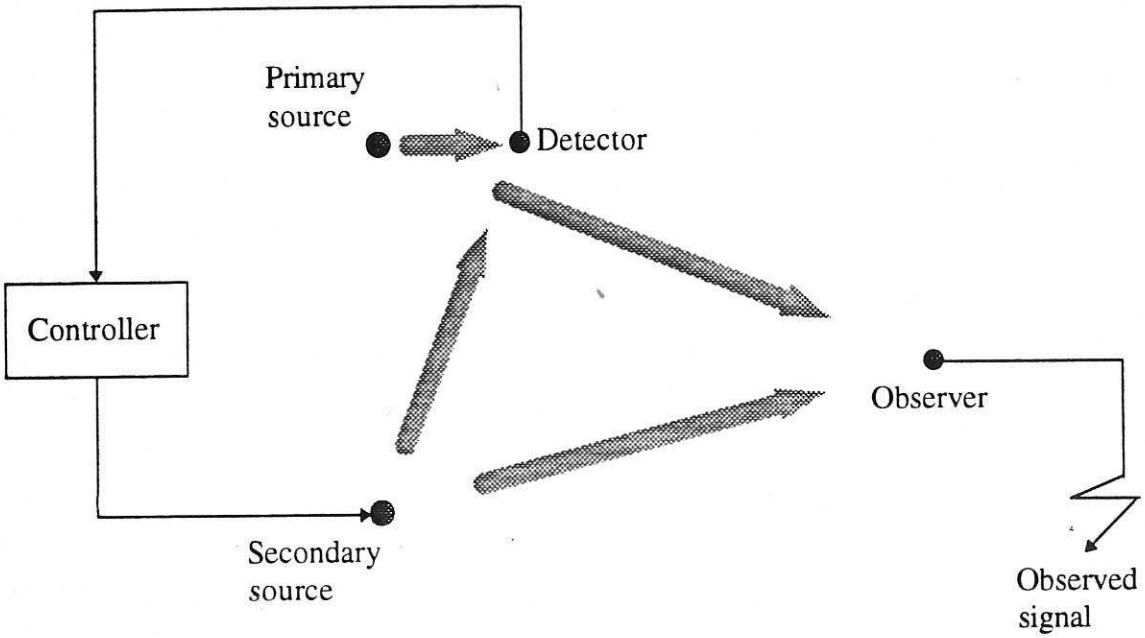

(a) Schematic diagram.

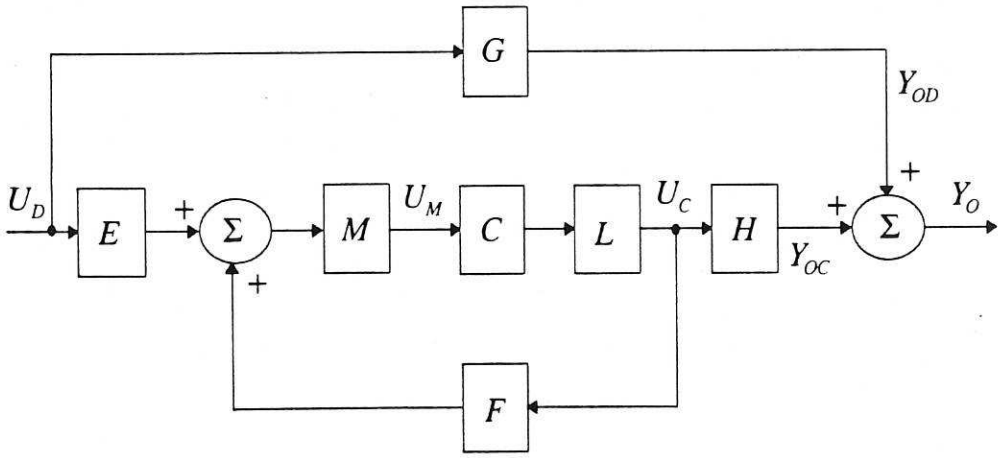

(b) Block diagram.

Figure 1: Active noise control structure.

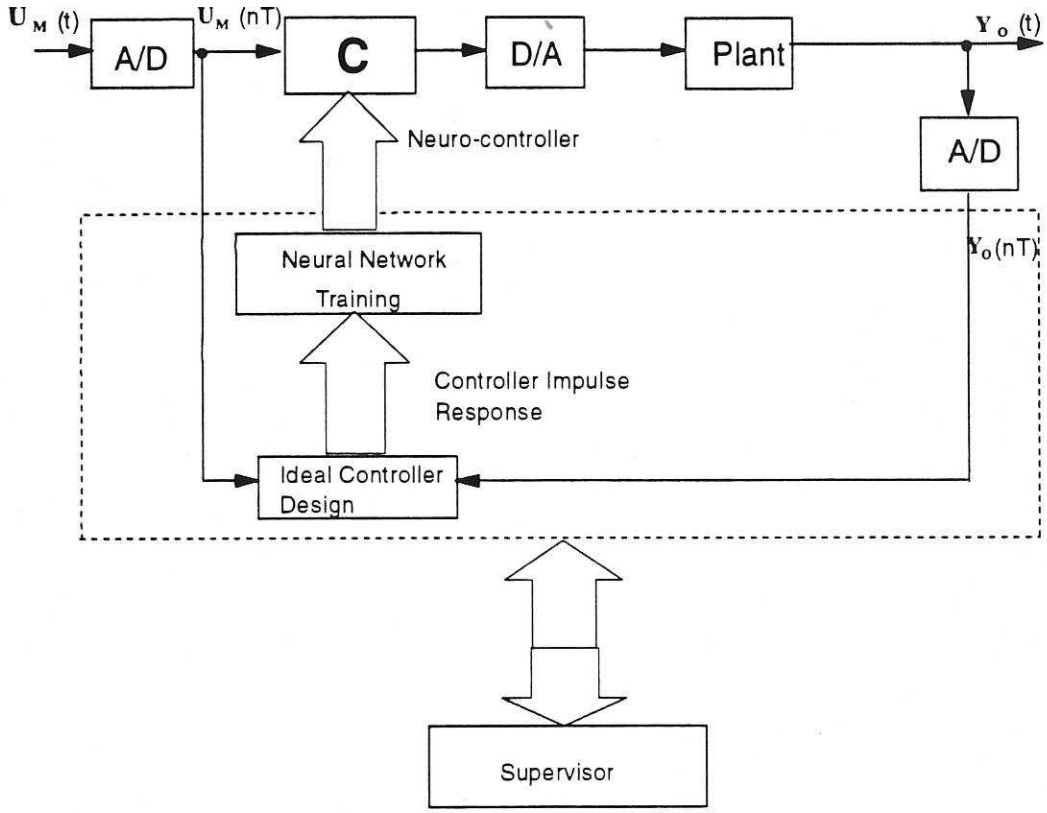

Figure 2: Neuro-self-tuning controller.

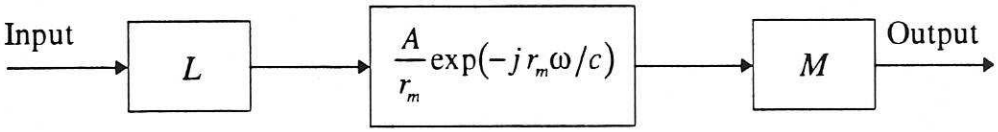

Figure 3: Frequency response measurement.

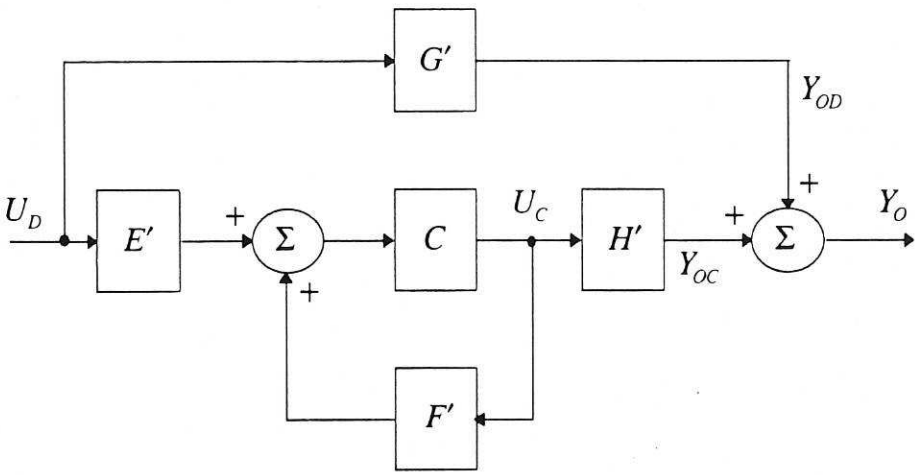

Figure 4: Block diagram of the simulated feedforward ANC structure.

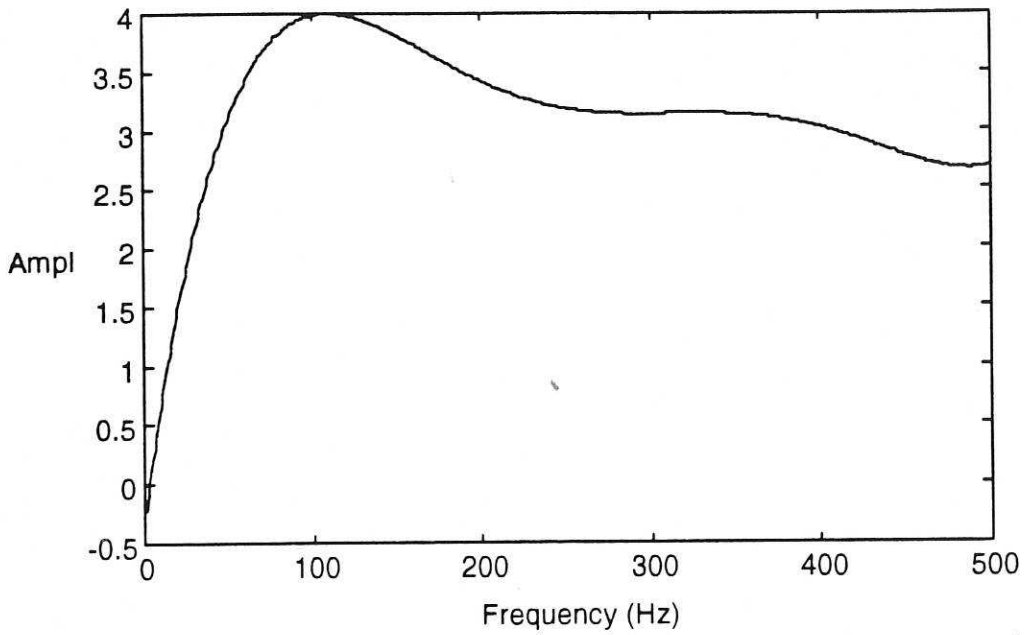

(a) System gain.

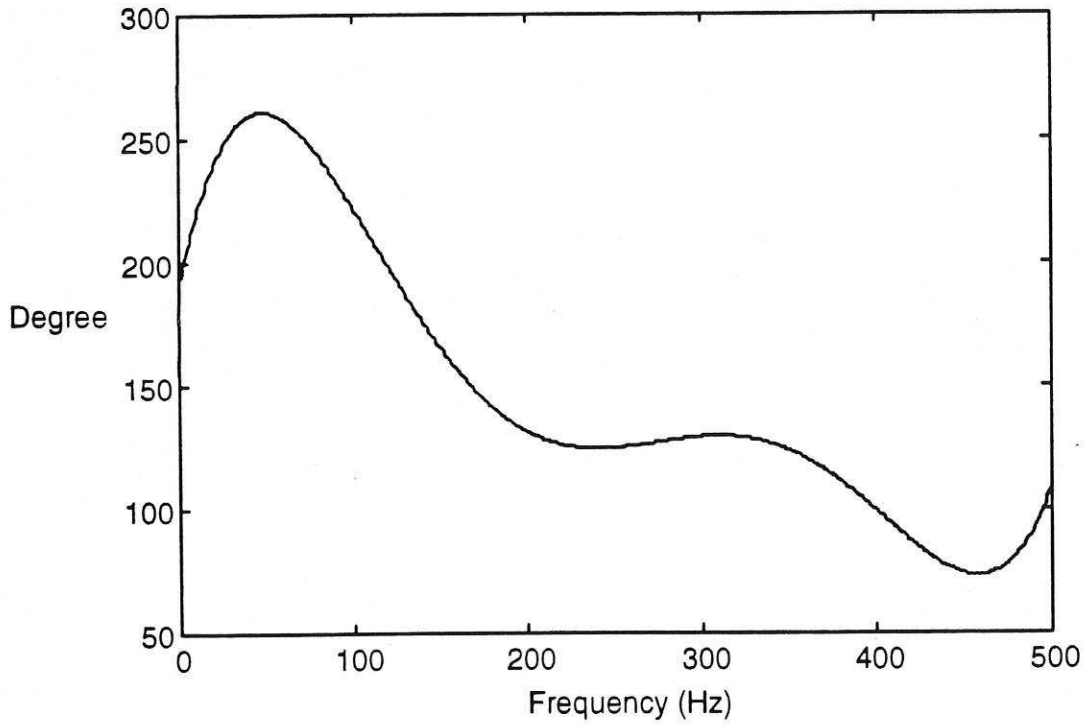

(b) System phase.

Figure 5: Transfer characteristics of loudspeaker-microphone combination.

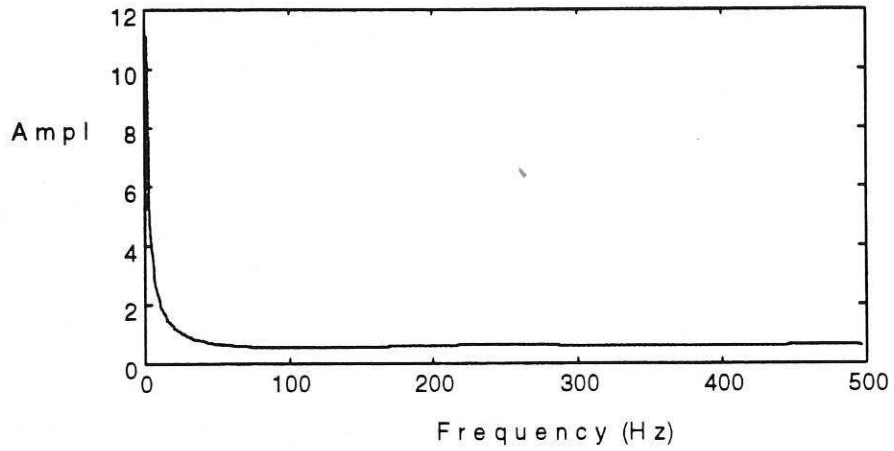

(a) Amplitude.

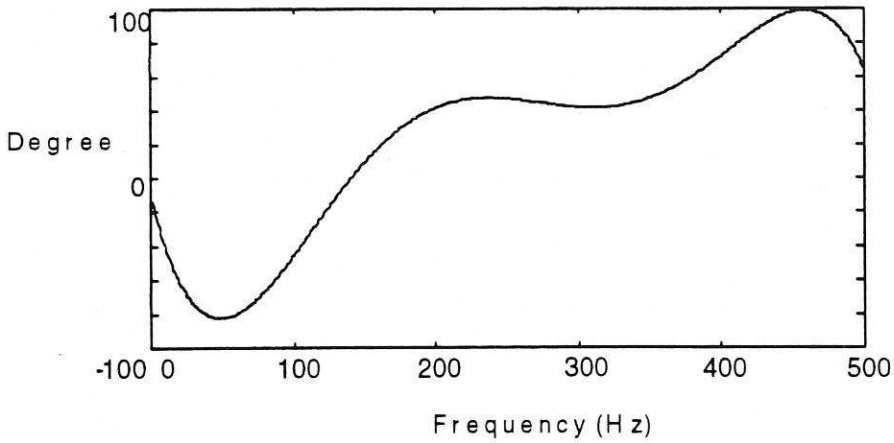

(b) Phase.

Figure 6: Transfer characteristics of the ideal controller.

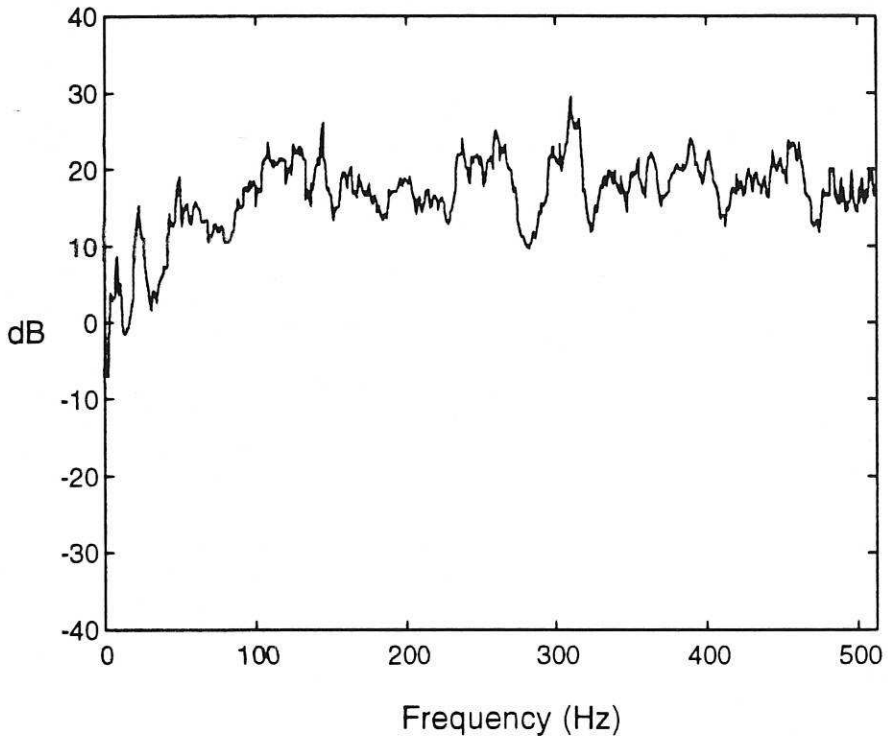

Figure 7: The cancelled spectrum with the ideal controller.

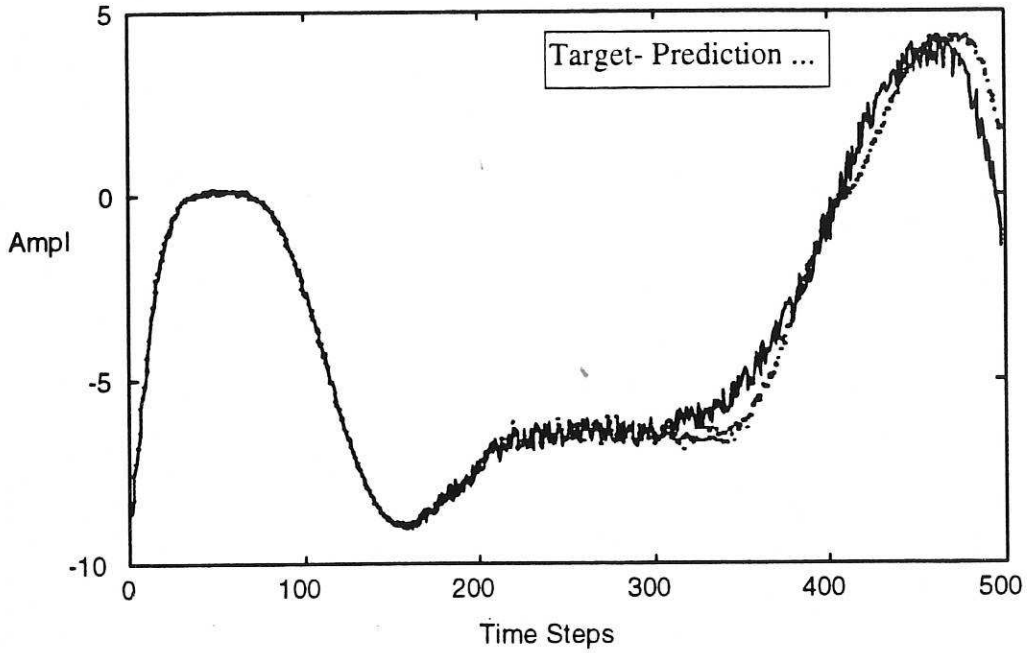

(a) One-step-ahead prediction.

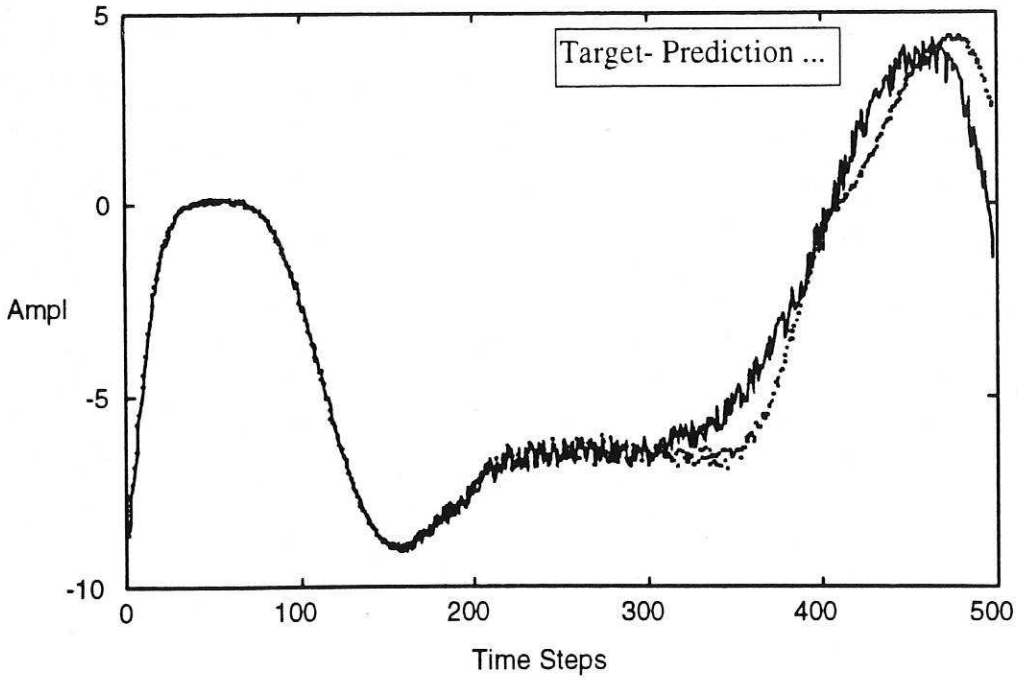

(b) Model predicted output.

Figure 8: Output prediction of the RBF neuro-controller.

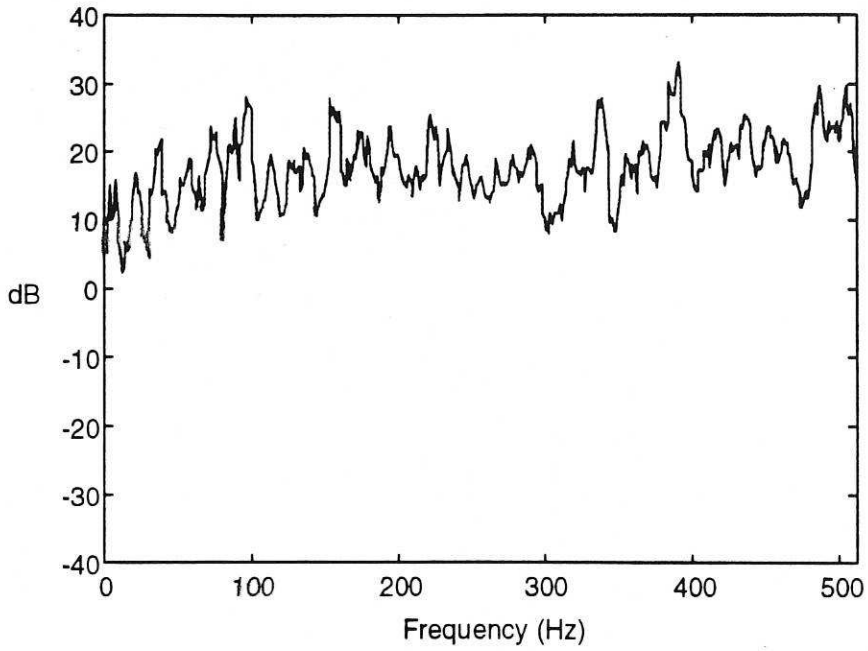

Figure 9: The cancelled spectrum with the RBF neuro-controller.